Ion-Excited Germanium L-Series X-Ray Spectra

P. G. Burkhalter, A. R. Knudson, and D. J. Nagel
Naval Research Laboratory, Washington, D.C. 20390
(Received 29 December 1972)

The Ge $L\alpha_{1,2}$ and $L\beta_1$ spectra obtained by ^{4}He ion bombardment at 3.0 and 5.0 MeV have major satellite peaks which correspond in energy with those appearing in photon- or electron-excited spectra. Many new satellite peaks can be observed in the ion-induced spectra because of enhanced multiple-vacancy production. An interpretation based on Hartree-Fock-Slater calculations for multiple $3d$ vacancies gives over-all good agreement for the observed satellite groups for both $L\alpha_{1,2}$ and $L\beta_1$ spectra; however, multiplet calculations are necessary to identify the various satellite components. The continous satellite structure produced by ^{20}Ne bombardment on Ge at 3.0, 5.0, and 10.0 MeV shows strong self-absorption effects. Published absorption data and variable-take-off-angle experiments were both used to correct for self-absorption. Satellite peaks occur at energies corresponding to multiple $(3d)^n$ plus N-shell vacancies where n has values of 4, 5, and 6. Satellite lines have also been identified corresponding to production of $(2p)^2$ vacancies by neon bombardment.

I. INTRODUCTION

Ion excitation produces intense x-ray satellite spectra because of the high probability of creating multiple vacancies. The purpose of this work was to advance the interpretation of L-series x-ray satellite spectra taking advantage of the high multiple-vacancy production with both light- and heavy-ion bombardment. Spectral measurements of Ge x rays with helium and neon excitation in the 3–10-MeV energy range were made with a high-resolution crystal spectrometer. The configurations and x-ray energies for the x-ray lines and energy levels pertinent to our study were obtained from Bearden[1,2] and are listed in Table I.

The x-ray satellite spectra produced by helium ions have major peaks which correspond in energy to those found in either photon- or electron-excited spectra[3–6] and also contain new satellite lines not previously seen. The L-series satellite spectra found with photon or electron excitation have previously been identified with a $3d$ vacancy, arising from $L_{\rm I} \rightarrow L_{\rm II,III} M_{\rm IV,V}$ Coster–Kronig (CK) transitions, in addition to the $2p$ vacancy which produces the parent x-ray lines. Good correlation between experimental and theoretical $L\alpha_{1,2}$ and $L\beta_1$ satellite spectra for $Z = 37$–56[7] and $Z = 42$[8] has been achieved with multiplet calculations using j-j and intermediate coupling assuming an initial $3d$ plus $2p$ vacancy configuration. Similar calculations have had partial success in predicting the peaks found in the Ge $L\alpha_{1,2}$ and $L\beta_1$ satellite spectra.[3] Hartree-Fock-Slater (HFS) calculations have previously been used in correlating aluminum $K\alpha$ and $K\beta$ satellite lines excited by nitrogen ions with multiple L-shell vacancy configurations.[9] In the present work, HFS calculations are used to correlate the helium-excited satellite lines from Ge with multiple M- and N-shell vacancies.

The Ge L spectra excited by energetic neon ions are dominated by multiple vacancies and show evidence of self-absorption at the $L_{\rm III}$ edge as was previously observed in heavy-ion L spectra of transition elements.[10] An L-shell hypersatellite arising from a double $2p$ vacancy in the initial configuration is apparent after correction for self-absorption.

II. EXPERIMENTAL CONDITIONS

Ion beams from the 5-MV Naval Research Laboratory Van de Graaff were used to excite Ge L x-ray spectra. The target used was a thick Ge crystal positioned at 45° to the incident-ion beam. X rays were measured at 90° to the beam using a computer-controlled flat-crystal Bragg spectrometer with a commercial 0.07°-divergence entrance collimator, an ammonium dihydrogen phosphate (ADP) crystal ($2d$ spacing = 10.642 Å), and a flow-proportional detector. The P-10 gas-flow detector

TABLE I. Germanium L-series x-ray transitions and energy levels.[a]

X-ray line	Designation	Energy (eV)
$\alpha_{1,2}$	$L_{\rm III}M_{\rm IV,V}$	1188.00
β_1	$L_{\rm II}M_{\rm IV}$	1218.5
β_3	$L_{\rm I}M_{\rm III}$	1294.1
β_4	$L_{\rm I}M_{\rm II}$	1286.1
Atomic level		**Energy (eV)**
$L_{\rm I}$		1414.3
$L_{\rm II}$		1247.8
$L_{\rm III}$		1216.7
$M_{\rm I}$		180.0
$M_{\rm II}$		127.9
$M_{\rm III}$		120.8
$M_{\rm IV,V}$		28.7

[a]References 1 and 2.

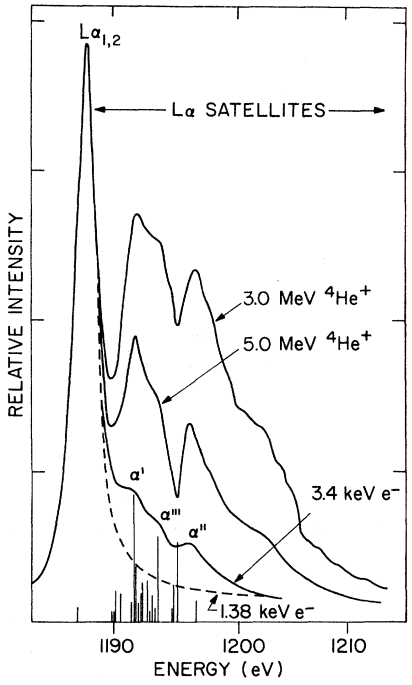

FIG. 1. Germanium $L\alpha_{1,2}$ spectra excited by 3.0- and 5.0-MeV helium ions, along with 1.38- and 3.4-keV electron-excited data and multiplet calculations by Blokhin *et al.* (Ref. 3). The spectra are normalized to the same intensity at the $L\alpha_{1,2}$ peak.

had a stretched polypropylene window (about 1 μ thick).

III. HELIUM-EXCITED DATA

A. Results

The Ge $L\alpha_{1,2}$ spectra obtained with 3.0- and 5.0-MeV helium-ion excitation are shown in Fig. 1 superimposed on the electron-excited spectra and multiplet calculations of Blokhin *et al.*[3] Likewise, the Ge $L\beta_1$ spectra excited in the same manner are plotted in Fig. 2. These spectra are relative x-ray intensities uncorrected for crystal-reflection efficiency, detector window absorption, and sample self-absorption effects. The crystal response for ADP is flat within 10% over the limited energy range used in this work, and the detector window absorption changes less than a few percent. The entire $L\alpha_{1,2}$ satellite structure is below the Ge L_{III} absorption edge. The $L\beta_1$ parent line and β_1 satellites lie between the L_{III} and L_{II} absorption edges. Therefore, the entire $L\beta_1$ spectrum is reduced in intensity because of self-absorption of x rays emitted by the thick target. Because the counting statistics for He excitation were not sufficient to identify individual components of these satellites, the intensities obtained by step scanning were smoothed with a five-point parabolic function to yield smooth envelopes for the low-intensity–high-energy satellites. The helium data were normalized to the intensity and energy of the $L\alpha_{1,2}$ and $L\beta_1$ parent lines of the electron-excited data. The electron-excited satellites are identified by conventional nomenclature for L-series x-ray peaks in the atomic-number range $Z \leq 32$. Blokhin *et al.*[3] presented direct experimental evidence that L-series satellites arise from excitation of the L_I level and subsequent L-shell CK transitions producing M-shell vacancies. They found that satellites were generated by either photon or electron excitation with incident energies above the L_I level, such as with Al $K\alpha_{1,2}$, but were not excited by Mg $K\alpha_{1,2}$ photons which are about 150 eV below the Ge L_I level. The vertical lines at the bottom of Figs. 1 and 2 represent the expected energies and intensities of x-ray satellites calculated by multiplet theory[3] for a Ge ion with a $2p$ and a $3d$ vacancy.

The enhanced satellite intensities obtained for both the 3- and 5-MeV helium excitation indicate the presence of additional satellites which are not found in the electron spectra because of lack of satellite intensity. In particular, the α' and α''' satellites appear as maxima of a cluster of satellites in agreement with the multiplet calculations. There are also clusters of higher-energy satellites seen for the first time in this Z range. Another difference between ion and electron excitation was

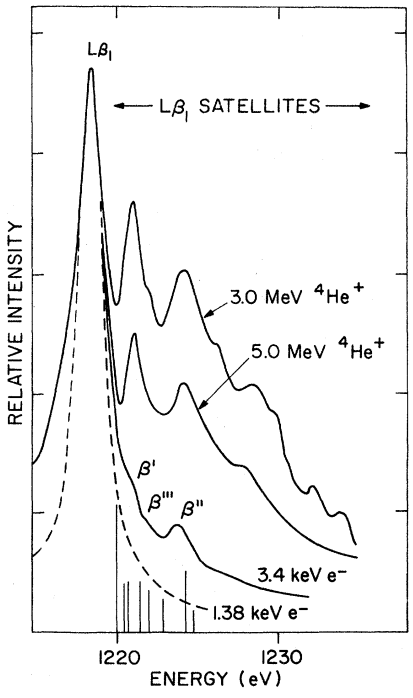

FIG. 2. Germanium $L\beta_1$ spectra excited by helium ions superimposed on electron-excited data and multiplet calculations by Blokhin *et al.* (Ref. 3). The spectra are normalized to the same intensity at the $L\beta_1$ peak.

TABLE II. Comparison of Ge $L\alpha_{1,2}$ and $L\beta_1$ satellite energies in eV relative to the parent line.

	Present work, ^{4}He	Blokhin[a] electron	Gwinner[b] photon	Lucasson[c] photon
α'	3.3	3.6	3.3	3.2
α'''	5.4	5.4	5.1	4.4
α''	8.5	8.0	8.1	7.5
β'	2.5	2.6	2.5	2.1
β'''	3.5	3.8		3.8
β''	5.6	5.2	5.8	5.1

[a]Reference 3. [b]Reference 4. [c]Reference 5.

a decrease in satellite-to-parent intensity ratios as the ion energy was increased. The ratio of the integrated $L\alpha'$, α''', α'' satellite group to the $L\alpha_{1,2}$ parent line intensity was 280% at 3.0 MeV and 140% at 5.0 MeV compared to a value of 38% for Blokhin's electron-induced data at 3.4 keV.

The energy spacings between satellite and parent lines for the three major satellite peaks in the 3-MeV data were obtained by computer unfolding with Gaussian peak shapes.[11] The experimental resolution at half-maximum intensity was 0.6 eV and the peak positions for the major satellites which appear as single peaks were determined to within ±0.2 eV. The energy spacings resulting from helium excitation are compared in Table II with results using photon or electron excitation. There is reasonable agreement for the major satellite peak-energy spacings for the three modes of excitation.

B. Discussion

A question that arises is whether or not new satellites appear with ion excitation; that is, do the same multiple-vacancy configurations occur regardless of the method of excitation? The L-series satellite lines found with photon- or electron-excitation result from ionization of the $L_{\rm I}$ level and subsequent CK transitions. According to McGuire, 94% of the $L_{\rm I}$ vacancies decay by CK transitions. Both $L_{\rm I} \rightarrow L_{\rm II}M$ and $L_{\rm I} \rightarrow L_{\rm III}M$ CK transitions have a high probability for exciting $3d$ vacancies, but some $3p$ vacancy production also occurs. On the other hand, the L-series satellite intensity enhancement found with light ion excitation is believed due to direct simultaneous L- and M-shell ionization, a situation similar to the simultaneous K- and L-shell vacancy production observed in aluminum $K\alpha$ satellite spectra excited by protons and helium ions.[12] Approximate calculations indicate that the peaks of the M-shell ionization cross sections should occur at 0.2, 0.9, and 1.3 MeV, respectively, for the $3d$, $3p$, and $3s$ subshells. Therefore, the satellite-to-parent intensity ratio is predicted to decrease with increasing helium energy in the 3- to 5-MeV region. This is in accord with the experimental data. Hence, simultaneous ionization of the L shell and any of the M subshells, including the $3s$, is possible with helium bombardment.

The experimental agreement in energy separation between major satellite peaks for both electron and helium excitation, which implies that essentially the same satellites are produced in the two cases, can be explained by considering various L- and M-shell transition rates. According to McGuire's[13,14] calculations the CK rate for M-shell vacancies is about six times the rate at which $2p$ vacancies are filled. Hence for both electron and helium excitation, most M-shell vacancies will be transferred to the $3d$ subshell before an L x ray is emitted, resulting in similar structure for the major satellites with both electron and helium excitation. However, multiple M-shell ionization occurs more frequently and results in observable higher-energy satellites with helium excitation. Also, N-shell vacancies may follow from M-shell CK transitions with helium excitation, but shifts due to individual N-shell vacancies are not discernible.

To give further support for the agreement of the major Ge x-ray satellites with electron and helium excitation and to aid in the classification of L-series satellites we have prepared semi-Moseley plots for both $L\alpha_{1,2}$ and $L\beta_1$ experimental x-ray satellite data. Experimental measurements of L-series x-ray satellites were extensively made in the 1930's at higher Z, in investigating the CK dependence on Z, and also at lower Z, starting at Ge, for transition elements. The square root of the experimental $L\alpha_{1,2}$ and $L\beta_1$ satellite energies relative to the parent lines are given in semi-Moseley plots as a function of Z in Figs. 3 and 4. It is known that nearly linear relations exist for L-series x-ray satellites in the Z range 37–55 in semi-Moseley plots. It was desirable to determine how Ge satellite spacings agree with those in x-ray spectra for both higher- and lower-Z elements. The $L\alpha_1$ satellite separations of Richtmyer and Richtmyer[15] and those of Randall and Parratt[16] were found to be nearly in agreement, and therefore, average values for these data were plotted in Fig. 3 for $L\alpha$ satellites. The data of Moore[17] for $Z = 36$ are also shown. The data for higher atomic numbers were smoothly extrapolated to meet the Ge data measured by both photon and ion excitation. The extrapolations were made by assuming correspondence in intensity between the Ge satellites and those of higher Z. The more-intense satellites at higher Z are α_4, α_5, and α_6. The satellite α_3 decreases in intensity as Z decreases and, following Pincherle,[7] α_3 may be taken as a composite of several $L\alpha_2$ satellites which may then combine with α_4 as the separation of $L\alpha_1$ and $L\alpha_2$ diminishes at lower Z. However, the extrapolation of satellite ener-

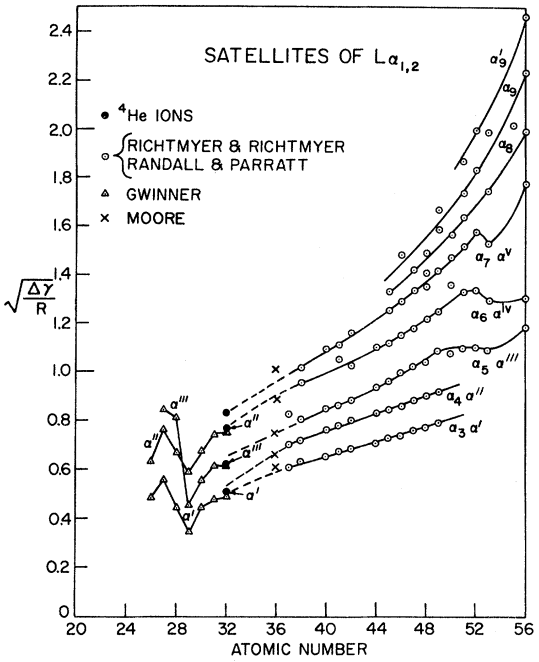

FIG. 3. Semi-Moseley plot of $L\alpha_{1,2}$ satellites together with the energy spacings for the 3.0-MeV helium-excited data.

gies and intensities may not be valid, because j-j coupling applies in the higher-Z region and intermediate coupling applies in the region which includes Ge. This suggests the need for further theoretical and experimental work in this region. Below $Z = 29$, we note considerable crossing of satellite energy spacings for elements containing unfilled $3d$ levels. In Fig. 4, the two most-intense $L\beta_1$ satellites found at higher Z extrapolate nearly exactly to the values for Ge $L\beta'$ and $L\beta''$, and join well with satellite separations for $Z = 30$.

It is valuable to associate the Ge L-satellite spacings with those for higher-Z elements because of the success in identification of x-ray satellites with multiplet components calculated for higher-Z elements. The satellite structure of $L\alpha_{1,2}$ for Au was calculated by Richtmyer and Ramberg[18] in the j-j coupling approximation for the transition $(2p_{3/2})(3d) \rightarrow (3d)^2$. The multiplet structure consists of 29 levels. Similarly Pincherle[7] has calculated L-series x-ray satellites spacings and transition probabilities for $L\alpha$ and $L\beta$ satellites with atomic-number range $Z = 37$–56. For these calculations, an additional vacancy in the M_{IV} or M_V shell—i.e., the $3d$ shell—is assumed because of the identification of L-series satellites with the Coster-Kronig effect. The calculations predict the correct overall satellite structure for relative energy spacings and transition probabilities, but the calculations yield too large satellite-to-parent energy spacings.

More recently, Demekhin[8] has successfully explained the $L\alpha_{1,2}$ and $L\beta_1$ satellite spectra for Mo ($Z = 42$) using multiplet calculations for energy spacings and transition probabilities in intermediate coupling. In the Ge calculations of Blokhin,[3] multiplet calculations rather successfully predict the α' and α''' cluster but the strong α'' satellite is not predicted as well by the multiplet calculations (see Fig. 1). The most-intense line calculated for the $L\beta_1$ satellites does not agree with the β' satellite but the other lines calculated by the multiplet theory agree reasonably well with the electron- and helium-excited spectra (see Fig. 2).

In previous work involving Al K x-ray spectra excited by nitrogen ions,[9] we obtained good agreement for the energy spacings of the $K\alpha$ and β satellites with calculations for K- plus L-shell vacancies. The energy spacings were calculated as differences in the total binding energies for the initial and final atomic configurations using the HFS wave functions calculated by the Herman–Skillman program.[19] The calculated energy spacings for the K-series satellites agreed well with the centroid of the satellite group composed of multiplet structure. Similarly, the L-series satellites for Ge could be calculated for various configurations LM^n where n is the number of missing $3p$ or $3d$ electrons. The first satellite energy spacing for a $3d$ vacancy is 4.0 eV which lies between α' and α'''. In the Herman–Skillman program, no provision is made for different j values and therefore the same

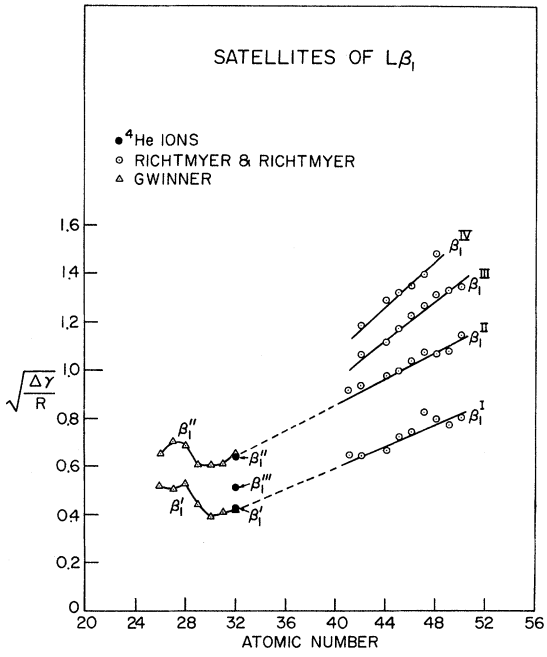

FIG. 4. Semi-Moseley plot of $L\beta_1$ satellites and 3.0-MeV helium-excited data.

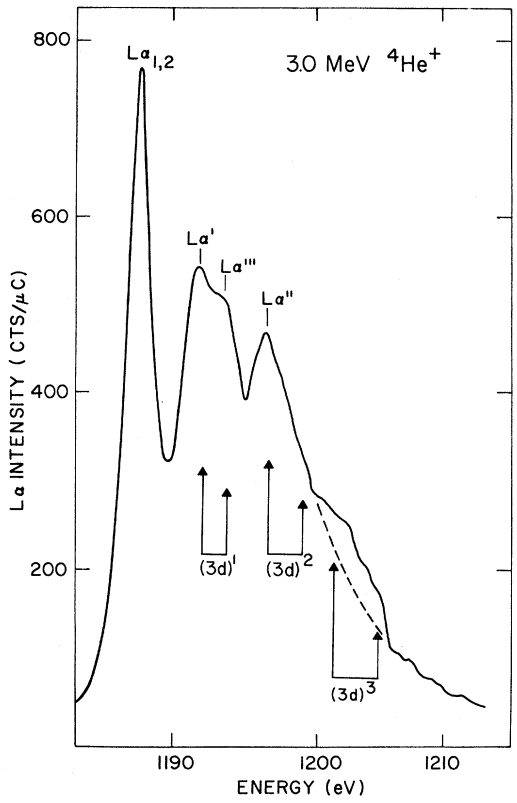

FIG. 5. Germanium $L\alpha_{1,2}$ spectrum excited by 3.0-MeV helium ions. The energy interval bracketed by a pair of vertical arrows is the change in satellite energy caused by removing all four N-shell electrons as calculated by the HFS method.

calculated spacings are used for the $L\alpha_{1,2}$ and $L\beta_1$ satellites. Calculations were performed for numerous L-, M-, and N-shell vacancy configurations for interpreting the helium- and neon-excited data and representative values are listed in Table III. The 3.0-MeV-helium data are presented again in Figs. 5 and 6 with arrows marking the energy spacings calculated for multiple $3d$ vacancies and for $3d$ plus the four N-shell electron vacancies. The HFS-calculated energy spacings agree reasonably well with the $L\alpha$ satellite intensity clusters.

An interesting question arises as to the origin of the intense $L\alpha''$ satellite which has a measured energy spacing 7.5–8.1 eV in photon- or electron-excited spectra, and a slightly larger 8.5 eV in the helium-excited data. The intensity of α'' would indicate correlation with a $(3d)^1$ vacancy, but the energy spacing agrees better with a $(3d)^2$ vacancy configuration according to the HFS calculations. The presence of a $(3d)^2$ satellite in the $L\alpha$ spectrum, and the apparent absence of a corresponding $L\beta$ satellite could be explained if the $L_{II} - L_{III}M_{IV,V}$ CK transition were allowed in Ge. Calculations by Chen[20] indicate that the $f_{2,3}$ probability is low but that Ge is a borderline element. Yin[21] found experimentally that the L_{II}:L_{III} photoelectron- and Auger-electron intensity ratios were nearly 1:2, indicating that the $L_{II} - L_{III}$ $M_{IV,V}$ CK transition is negligible and cannot account for the α'' intensity. Therefore α'' is believed to be intense in the helium-excited spectrum because it is a multiplet component of a $(3d)^1$ vacancy superimposed on some of the multiplet structures arising from $(3d)^2$ vacancy configurations. The larger energy spacing for α'' excited by helium, compared with the electron- and photon-excited spacings listed in Table II, results from enhanced $(3d)^2$ vacancy production with ions as indicated in Fig. 5.

The energy separation of a given $L\beta$ satellite is generally about two-thirds of the separation of the $L\alpha$ satellite bearing the same label. This appears to be a coincidence, since a different multiplet structure occurs for the $L\alpha$ and $L\beta_1$ satellites. The β' peak together with the β''' and β'' satellites of the $L\beta_1$ parent are believed to be multiplet components of a single $3d$ vacancy as proposed by Blok-

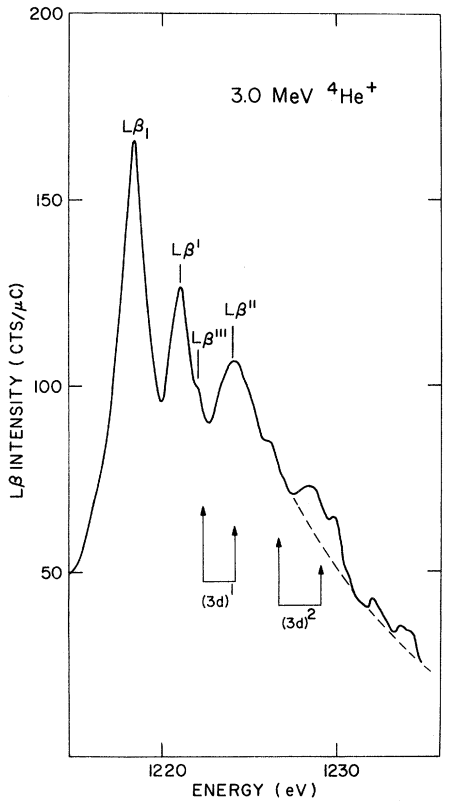

FIG. 6. Germanium $L\beta_1$ spectrum excited by 3.0-MeV helium ions. The energy interval bracketed by a pair of vertical arrows is the change in satellite energy caused by removing all four N-shell electrons as calculated by the HFS method.

TABLE III. Energy spacings in eV for various vacancy states in germanium calculated using HFS wave functions.

Vacancy state for $L\alpha_{1,2}$ satellite	Energy spacing from $L\alpha_{1,2}$ parent (eV)
$(4s)^2\ (4p)^2$	1.3
$(3d)^1$	4.0
$(3p)^1$	4.5
$(3d)^1$ + empty N shell	5.7
$(3d)^2$	8.4
$(3d)^2$ + empty N shell	10.8
$(3d)^3$	13.4
$(3d)^3$ + empty N shell	16.8
$(3d)^4$	19.0
$(3d)^5$	25.4
$(3d)^6$	33.0
$(2p)^1$	49.5
$(2p)^2$	99.2

hin. The HFS calculations approximately predict the centroid of these satellites as indicated in Fig. 6.

IV. NEON-EXCITED DATA

A. Results

The Ge L x-ray spectra excited by 3- , 5- , and 10-MeV neon ions at 45° incident beam angle are shown in Fig. 7. The neon-excited Ge L spectrum is dominated by x rays from multiple-vacancy configurations. The satellite intensity increases rapidly with a shoulder at 1210 eV and an abrupt intensity decrease at the L_{III} absorption edge at 1217 eV. There is also an intensity bump at 1236 eV in each spectrum which could possibly be introduced by self-absorption. A broad higher-energy satellite peak occurs at 1320, 1335, and 1350 eV in the 3- , 5- , and 10-MeV data, respectively. Data were also collected at 30° and 60° incident angles to vary the amount of absorption of the emitted x rays for 3-MeV excitation. The peaks at 1236 and 1335 eV were present in all the spectra. The 1236-eV bump was more distinct at the lower incident angle indicating a real satellite peak whose intensity is strongly affected by self-absorption. The 5-MeV neon-excited Ge spectrum is replotted as the short-dashed curve in Fig. 8 together with a 5.0-MeV proton-excited Ge spectrum. The proton-produced spectrum is dominated by a single L-shell vacancy as in either electron- or photon-excited spectra. Also plotted in this figure are spectra corrected for self-absorption, which will be discussed later. To aid in the determination of the origin of the L spectra obtained with neon bombardment, we looked for K x rays by rotating the Ge target 90° and measuring the x-ray spectrum directly with a Si(Li) semiconductor detector. No evidence of K x rays was found in the 3.0-MeV neon-excited Ge spectra. Therefore, if the higher-energy peaks result from multiple L-shell vacancies, their origin is not KLL Auger emission as has been found in Ag L spectra,[22,23] but rather multiple L-shell excitation by the incident neon ion.

B. Discussion

The neon-excited spectra are essentially different from the helium-excited spectra because of the large number of M- and N-shell vacancies formed by the high-energy–heavy-ion collision. The satel-

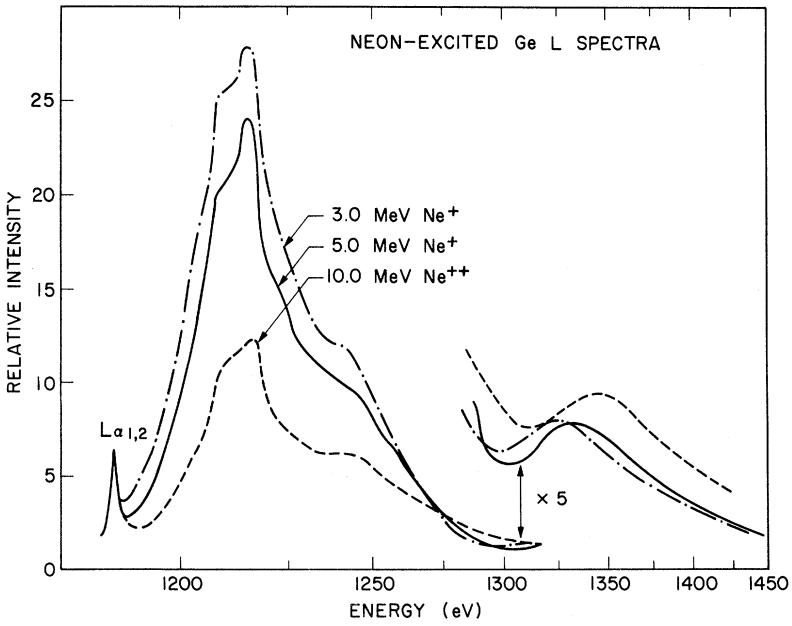

FIG. 7. Neon-excited Ge L spectra for 3-, 5-, and 10-MeV ion bombardment. The spectra are normalized to the same intensity at the $L\alpha_{1,2}$ line. One unit of relative intensity corresponds to approximately 10, 22, and 78 counts/6.25×10^{12} incident particles at 3, 5, and 10 MeV, respectively.

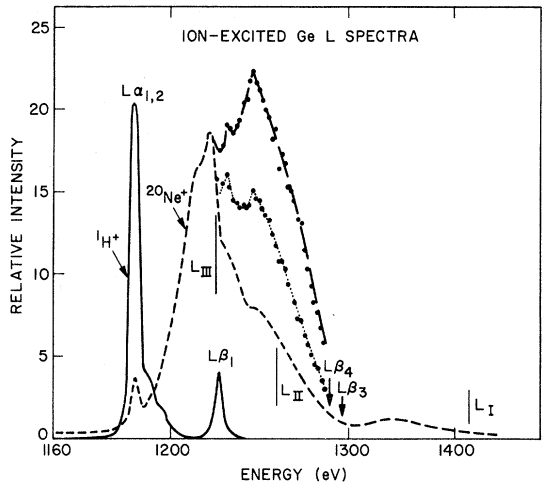

FIG. 8. 5.0-MeV proton- and neon-excited Ge L spectra. The long-dashed curve is for intensities corrected for self-absorption by using published L-absorption jump ratios, while the dotted curve was obtained applying self-absorption corrections from data collected at different target angles. One unit of relative intensity corresponds to 38 and 22 counts/6.25×10^{12} incident particles, respectively, for the proton- and neon-excited spectra.

lite structure extends over a broad energy range which includes the three L-shell absorption edges, and we find evidence of strong self-absorption at the L_{III} edge. In attempting to correct for self-absorption, large inconsistencies were found in published absorption coefficients. There is agreement within 20% for the absorption coefficients below the L_{III} edge and above the L_I edge, but poor agreement in the critical region between edges. For example, the value for the L_{III} jump ratio was measured as 1.5 for Ge by Blokhin[3] while the value for Ge obtained by extrapolation in the absorption-coefficient tables was 5.6.[24] Bonnelle[25] obtained 3.0 and 1.4 for the L_{III} and L_{II} jump ratios of Cu. Values of 3.15 and 1.4 were used for Ge L_{III} and L_{II} jump ratios together with the Ge absorption curve measured by Lucasson-Lemasson.[26] This curve was obtained by transmission measurements through a Ge foil. The transmission increased monotonically between the L_{III} and L_{II} absorption edges. Therefore self-absorption does not introduce the satellite bump at 1236 eV.

The average effective depth for x-ray production for 5-MeV neon ions in Ge was calculated to be 0.45 μ between the L_{III} and L_{II} edges and 0.40 μ between the L_{II} and L_I edges. The self-absorption corrected intensities were normalized to the peak-intensity value just below the L_{III} edge and plotted as the long-dashed curve in Fig. 8. The L_{III} jump ratio appears to have been a reasonable choice as the abrupt intensity change has been removed at the L_{III} edge.

A second method of performing absorption corrections was also used. In this method two measurements of the Ge L spectrum were made, one with the normal to the target surface at 30° to the incident beam and the other with the normal at 60°. The ratio of the intensity at a given spectrometer position in the 30° run to the intensity at the same position in the 60° run was calculated to produce a curve of intensity ratio as a function of spectrometer position or x-ray energy. This curve was found to be similar to the absorption curve obtained by Lucasson-Lemasson[26] for amorphous Ge. These data were obtained at 3 MeV due to the inability of the accelerator to reach 5 MeV at that time. Calculations of x-ray yields were performed for varying incident and take-off angles, including x-ray absorption in the target and assuming the x-ray-production cross section and the range of the ion depended on the ion energy through some power of the ion energy. The data of Northcliffe and Shilling[27] were used to determine the exponent for the dependence of the ion range on energy, and various exponents suggested by the present data were used for the dependence of the x-ray-production cross section on ion energy. These calculations were used to derive an empirical relationship between the 30° to 60° ratio at 3 MeV and the absorption correction for 45° incidence at 5 MeV. It was found that this relationship was relatively insensitive to large changes in the exponent assumed for the power-law dependence of the x-ray-production cross section. This gave some confidence that the accuracy of the correction to the 5-MeV data was not dependent on the accuracy of our assumptions about the depth distribution of the x-ray production. The resulting correction to the 5-MeV data is shown as the dotted curve in Fig. 8.

It can be seen that both self-absorption correction methods yield the same spectral features. The shoulder observed at about 1210 eV is identified as multiple $L\alpha_{1,2}$ satellites with a most-probable hole configuration of $(2p)(3d)^4$ plus a number of N-shell vacancies. The peaks on both sides of the L_{III} edge at 1216 and 1224 eV are also believed to be $L\alpha_{1,2}$ satellites with $(3d)^5$ and $(3d)^6$ vacancies plus N-shell vacancies being suggested by HFS calculations. The peak at 1236 eV is too strong to be a satellite of $L\beta_1$ and agrees within 4% with the calculated energy separation for an $L\alpha_{1,2}$ hypersatellite due to two $2p$ vacancies in the initial state. This is in contrast to the O^{4+} data of Der *et al.*[10] for Ni, Cu, and Zn L series which had intense peaks about 100 eV from the parent lines and were identified with $(2p)^2$ plus numerous M-shell holes.

The peak at about 1335 eV is broad and probably corresponds to satellites of the $L\beta_4$ and $L\beta_3$ lines with $(2p)^2$ and $(3d)^n$ vacancies. The shift toward

higher energy of the $L\beta_4$ and $L\beta_3$ satellites in the vicinity of 1335 eV is believed to be due to the increase in $(2p)^2$ vacancy production as the beam energy is increased. As the incident neon energy is increased, the satellite intensity between the $L\alpha_{1,2}$ line and the L_{III} absorption edge becomes smaller relative to the $L\alpha_{1,2}$ line, indicating less M-shell ionization. A rough estimate indicates that the $3s$, $3p$, and $3d$ ionization cross sections should peak at approximately 6.5, 4.5, and 1.0 MeV, respectively, which is in general agreement with the present data.

V. CONCLUSIONS

The enhanced satellite intensity with He excitation and the agreement in the major satellite peaks with photon and electron data suggest that a particle accelerator could advantageously be used to increase our knowledge of L-series x-ray satellites, particularly in those regions of the semi-Moseley plots where data are sparse. Higher-resolution measurements may also be of use in completing the empirical systematics and comparing experiment with theory; however, the present measurements approach the resolution limit set by the $2p$-vacancy lifetime.

L-series x-ray satellite spectra cannot be interpreted by HFS calculations alone because of overlapping multiplet structure. However, thorough tests of multiplet calculations using intermediate coupling for the $30 \leq Z \leq 40$ region must await more extensive experimental measurements. Calculations of multiplet structure and Coster-Kronig transition rates for multiple-vacancy states are also desirable.

A nearly continuous and complex L-series satellite spectrum, complicated by self-absorption, is produced by energetic heavy ions, such as Ne ions, in the 3- to 10-MeV range. The two absorption-correction approaches gave spectra which disagreed significantly in over-all intensity although they exhibit the same peak structure. It appears that self-absorption in heavy-ion excited x-ray spectra will be a significant nuisance in studies of high-energy collisions using solid targets.

[1]J. A. Bearden, Rev. Mod. Phys. 39, 78 (1967).

[2]J. A. Bearden and A. F. Burr, Rev. Mod. Phys. 39, 125 (1967).

[3]M. A. Blokhin, G. Zommer, V. F. Volkov, and L. M. Monastryrskii, Fiz. Tverd. Tela 11, 17 (1968) [Sov. Phys.-Solid State 11, 12 (1969)].

[4]E. Gwinner, Z. Phys. 108, 523 (1937).

[5]A. Lucasson-Lemasson, Compt. Rend. 248, 1156 (1959).

[6]R. D. Deslattes, Phys. Rev. 172, 625 (1968).

[7]L. Pincherle, Phys. Rev. 61, 225 (1942).

[8]V. F. Demekhin, A. P. Gangha, A. T. Kozakov, and I. Ya. Kudryavtsen, Izv. Vyssh. Uchelon. Zaved. Fiz. 154, 4 (1969). Naval Research Laboratory Translation No. 1239 is available.

[9]A. R. Knudson, D. J. Nagel, P. G. Burkhalter, and K. L. Dunning, Phys. Rev. Letters 26, 1149 (1971).

[10]R. C. Der, R. J. Fortner, T. M. Kavanagh, and J. M. Khan, Phys. Letters 36A, 239 (1971).

[11]P. G. Burkhalter, in *Applications of Low Energy X- and Gamma Rays*, edited by C. A. Ziegler (Gordon and Breach, New York, 1971), p. 147.

[12]A. R. Knudson, P. G. Burkhalter, and D. J. Nagel, in *Proceedings of the International Conference on Inner-Shell Phenomena*, edited by R. W. Fink (U.S.A.E.C., Washington, D. C., 1973), p. 1675.

[13]E. J. McGuire, Phys. Rev. A 3, 587 (1971).

[14]E. J. McGuire, Phys. Rev. A 5, 1052 (1972).

[15]F. K. Richtmyer and R. D. Richtmyer, Phys. Rev. 34, 574 (1929).

[16]C. A. Randall and L. G. Parratt, Phys. Rev. 57, 786 (1940).

[17]H. R. Moore, Proc. Phys. Soc. Lond. A70, 466 (1957).

[18]F. K. Richtmyer and E. G. Ramberg, Phys. Rev. 51, 925 (1937).

[19]F. Herman and S. Skillman, *Atomic Structure Calculation* (Prentice-Hall, Englewood Cliffs, N. J., 1963).

[20]M. H. Chen, B. Crasemann, and V. O. Kostroun, Phys. Rev. A 4, 1 (1971).

[21]L. I. Yin (private communication).

[22]C. Burbank, Phys. Rev. 56, 142 (1939).

[23]R. D. Richtmyer, Phys. Rev. 56, 146 (1939).

[24]Wm. J. Veigele, E. Briggs, L. Bates, E. M. Henry, and B. Bracewell, Report No. KN-71-431(R), p. 234, 1971 (unpublished).

[25]C. Bonnelle (private communication).

[26]A. Lucasson-Lemasson, Compt. Rend. 242, 3059 (1959).

[27]L. C. Northcliffe and R. F. Shilling, Nuclear Data A 7, 233 (1970).